Thermal treatment effect on structural and mechanical properties of Cr–C coatings

Mamoun Fellah, Linda Aissani, Amel Zairi, Mohamed Abdul Samad, Corinne Nouveau, Mohamed Zine Touhami, Hamid Djebaili, Alex Montagne, Alain Iost

Thermal treatment effect on structural and mechanical properties of Cr–C coatings

M. Fellah [a,b], L. Aissani[b,c], A. Zairi[d], M. Abdul Samad[e], C. Nouveau[f], M. Z. Touhami[b], H. Djebaili[a], A. Montagne[d] and A. Iost[d]

[a]Mechanical Engineering Department, ABBES Laghrour University, Khenchela, Algeria; [b]Tribology, Materials Surface and Interface, Laboratory of Foundry, BADJI Mokhtar University, Annaba, Algeria; [c]Physics Department, ABBES Laghrour University, Khenchela, Algeria; [d]Mechanical Surfaces and Materials Processing Laboratory, ENSAM Arts et métiers Paris Tech, Lille, France; [e]Mechanical Engineering Department, King Fahd University of Petroleum & Minerals, Dhahran, Saudi; [f]LaBOMaB ENSAM Arts et métiers Paris Tech, Cluny, France

ABSTRACT

In the present study, the effect of thermal treatment on the mechanical and structural properties of chromium carbide coatings with different thicknesses is evaluated. The coatings were deposited by cathodic magnetron sputtering on XC100 steel substrates. Samples were annealed in vacuum, at different temperatures ranging from 700 to 1000°C for 1 h, resulting in the formation of chromium carbides. X-ray diffraction (XRD), microanalysis X/energy-dispersive X-ray spectrometer (EDS), X-ray photoelectron spectroscopy (XPS) and scanning electron microscopy analysis were used to characterise the samples. Mechanical properties were evaluated by nano-indentation tests and the residual stress was calculated with the Stoney formula. The XRD analysis suggests the formation of the Cr_7C_3, $Cr_{23}C_6$ carbides at 900°C. For thin films, they transformed totally to ternary $(Cr, Fe)_7C_3$ carbides and their partial transformation has been observed in the case of thick films at 1000°C, without the formation of Cr_3C_2. The EDS and XPS showed the diffusion mechanism between the chromium film and the steel substrate for the Cr, Fe, C, O elements during the annealing treatment. The increase of chromium film thickness from 0.5 to 2.64 µm, contributed to the significant enhancement of mechanical properties such as hardness (H) (from 12 to 26.3 GPa) and Young's Modulus (E) (from 250 to 330 GPa), respectively.

KEYWORDS

Chromium carbide; hardness; Young's modulus; annealing treatment; diffusion

1. Introduction

During the last decade, transition metal carbides and nitrides with good mechanical properties have started to make their mark in surface engineering.[1] They have attracted much attention due to their excellent mechanical and physical properties such as high hardness (about half that of diamond), high melting temperature, high chemical and thermal stability, good wear and corrosion resistance.[2] The hard chromium carbide coatings produced by physical vapour deposition,[3] chemical vapour deposition[4] or by means of electrodeposition techniques[5,6] with a few microns thickness, have enhanced the mechanical resistance of various parts. For example, Zhou *et al.*[7] discovered that chromium and ternary chromium carbide films are effective in protecting steel and various alloys from chemical attack.

At present, it's considered the best choice, in various industrial applications. Recent results from Castillejo *et al.*[8] and Aissani *et al.*[9] showed that chromium-based coatings, because of their high wear resistance and hardness, can be used for steel protection for sliding bearing applications etc. In general, chromate conversion coatings produced on various metals by chemical or electrochemical treatment with mixtures of chromium hexavalent compounds and certain other compounds are soft and gelatinous when freshly formed, but become harder once dried or aged.[10] The effect of thermal treatments on the mechanical properties of interference films electrochemically deposited on stainless steel has been investigated by Poletika *et al.*[11]

However, the possibility of using the steel substrate itself as a source of carbon, in order to create very coherent hard chromium carbide coatings by means of a diffusion and transformation process has not been investigated comprehensively. Hence the main focus of the present study is to evaluate the above feasibility and also to investigate the influence of annealing treatment and the film thickness on the chemical composition, structure, surface morphology and mechanical properties of the Cr/XC100 samples.

2. Experimental details

Chromium (Cr) thin films were deposited in a high vacuum system with a base pressure of 2×10^{-5} Pa by radio frequency (R.F) magnetron sputtering (NORDIKO type 3500. 13.56 MHz) in a pure Argon atmosphere on Si (100) wafers (10×10 mm^2, 380 µm thick) and polished XC100 steel discs (15 mm diameter and 3 mm thick). A Cr (99.95 at.-%) target with a diameter of 10.16 cm and mounted in an off-axis configuration with a substrate-to-target distance of 8 cm and 45° from normal was used to deposit the Cr films. The typical composition of XC100 steel is: (0.95–1.05) wt-% C, (0.5–0.8) wt-% Mn, 0.05 wt-% S, 0.25 wt-% Si, 0.035 wt-% (P and S), with Fe as the balance. The substrates were ground, polished and ultrasonically cleaned for 5 min (each successively in trichloroethylene, methanol and acetone) to an average roughness (Ra) of 30 ± 0.01 nm (measured by an atomic force microscope). Before deposition, the substrates were bombarded with Ar^+ ions for 5 min at −700 V and at 1 Pa to clean them of any contaminants and oxide films. During deposition, the substrate temperature was estimated to be around 150–200°C. The Cr

target was also cleaned with an Ar^+ discharge for 5 min at 250 W (−500 V) and a working pressure of 0.1 Pa. The substrates were coated with a 230–250 nm thick Cr under-layer before the actual deposition of the coatings to improve the adhesion. Coatings with different Cr thicknesses were obtained by varying the deposition time between 5 and 120 min at 650 W (−900 V). After deposition, samples with 0.5, 1.13 and 2.46 µm thick films (measured as given below) were obtained at 30, 90 and 120 min, respectively. The samples were then annealed between 700 and 1000°C for 1 h at a pressure of 0.4 Pa. The structural analysis was conducted by X-ray diffraction (XRD) in a SIEMENS D500 system, with a CoK_α radiation (30 kV, 50 mA, $\lambda_{Co} = 0.178$ nm, the step size was 0.05° 2θ with 0.02 s/step). The average crystallite size of the thin films was determined by Scherrer's method: [9]

$$D = \frac{0.9\,\lambda}{\beta.\cos\theta} \quad (1)$$

where 0.9 is the shape factor, λ represents the X-ray wavelength used for the measurement ($\lambda_{Co} = 0.178$ nm), β is the line width (FWHM) in radians and θ is the Bragg angle.

The lattice parameter of the Cr_7C_3 phase was determined by the Bragg formula. The position of Cr_7C_3 (202) diffraction peak was used to estimate the crystallite size and lattice parameter. The surface morphology and the thickness of the coatings were determined by a scanning electron microscopy HR-SEM system which was equipped with an energy-dispersive X-ray spectrometer (EDS, Oxford INCA x-act)) to determine their chemical composition.

X-ray photoelectron spectroscopy (XPS, Riber SIA 100) analysis was also performed to verify the chemical composition of the coatings; the XPS chemical composition was estimated from the peak areas of the core level: C Is and Cr 2p by Al Kα X-rays. The film surface roughness was measured by atomic force microscopy (Nano-scope V).

Before the annealing treatment, the compressive residual stresses (σ) of the films were calculated by Stoney's formula[9] for coatings deposited on Si substrates.

$$\sigma = \pm \frac{E_s}{6\,(1-\nu_s)} \times \frac{e_s^2}{e_f}\left(\frac{1}{R} - \frac{1}{R_0}\right) \quad (2)$$

where σ is the residual stress in the thin film, E_s and ν_s are Young's Modulus (195 GPa) and Poisson's ratio (0.29) of the substrate, e_f and e_s indicate the film and substrate thicknesses, respectively, R is the curvature radius of the sample after deposition, and R_0, the curvature radius before deposition.

The hardness and Young's Modulus of the coatings were measured by nano-indentation (MTS-XP) in continuous stiffness mode, where the tip oscillates with a frequency of 45 Hz and an amplitude of 2 nm. A diamond Berkovich indenter with a tip radius of about 200 nm was used in the experiments with a maximum load of 10 mN. The loading and unloading phases of the indentations were carried out under load control at a nominal rate of 0.05 mN s^{-1}.

The hardness and Young's modulus of the coatings were calculated using the Oliver and Pharr method.[12] The reported values were determined from an average of five indentations and were evaluated at a depth of 10% of the total film thickness, in order to avoid the influence from the steel substrate and/or the surface roughness.

3. Results and discussion

3.1. Microstructure and chemical composition

XRD patterns of chromium films before and after annealing treatment (900 and 1000°C) at three different thicknesses are presented in Figure 1. It can be observed that, before annealing, in addition to the substrate peaks ((110), (200) and (211) of Fe_α (JCPDS65-4899), (211) and (120) of Fe_3C, (JCPDS 035-772), the deposited films are constituted of pure chromium with (110) Cr diffraction peak at 51° (JCPDS 6-694) and (110) and Cr_2O_3 (200) diffraction peaks at 42 and 44.3°, respectively, (JCPDS 85-0869) (Figure 1). The thermal treatment of the samples between 700 and 800°C exhibited the same results as found before annealing.

However, after annealing treatment of the three samples in the experimental temperature range (900–1000°C), significant changes in the XRD pattern (Figure 1) were observed. The reason probably was the addition of carbon to pure chromium by diffusion which encourages the formation of carbides in the film solidification structure.[13] The presence of the Cr_7C_3 phase may be indicative of a low stability of pure chromium at high annealing temperatures. It can be clearly seen that the binary carbide Cr_7C_3 with an orthorhombic

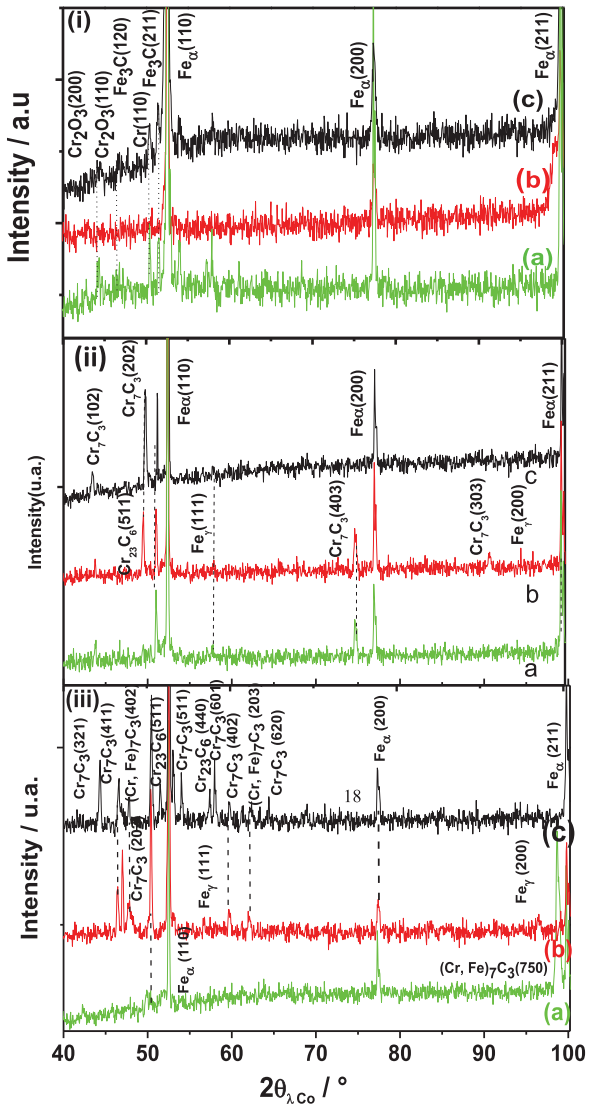

Figure 1. XRD patterns of (i) 0.5 µm Cr/XC100, (ii) 1.13 µm Cr/XC100 and (iii) 2.64 µm Cr/XC100. (a) as deposited, (b) after annealing at 900°C for 1 h and (c) after annealing at 1000°C for 1 h.

structure, forms at 900°C with (200) and (101) planes at 44.31 and 47.96° (JCPDS 006 0683), respectively, in all films and grows in plane numbers and intensity with increase of annealing temperature at 1000°C.

It is also observed that the binary carbide Cr_7C_3 is totally transformed into ternary carbide $(Cr, Fe)_7C_3$ in the thin film (0.5 µm Cr/XC100) with the disappearance of (101) and (200) Cr_7C_3 planes and the appearance of (750) and (402) $(Cr, Fe)_7C_3$ planes at 50.37 and 98.7° (JCPDS (005 0720), respectively. However, this transformation is partial in both 1.13 µm Cr/XC 100 and 2.64 µm Cr/XC100 films at 1000°C. This means that Fe diffused from the substrate into the coated films and reacted with Cr_7C_3 forming ternary carbides at a temperature of 1000°C. The formation of binary (Cr_7C_3) and ternary carbides ($(Cr, Fe)_{23}C_6$) mixture was also observed at high, annealing temperatures of 1000°C, in the chromium carbides powder.[14,15]

Ternary $(Cr, Fe)_7C_3$ carbide was formed also with eutectic matrix in the Fe–Cr–C hard facing coatings.[7] On the other hand, the Cr23C6 is revealed only at 900°C in all Cr films at 51.53° by (511) plane, (JCPDS 035 0694), and developed by the appearance of (440) plane orientation in the 2.64 µm Cr/XC100 coating at 1000°C. In the case of films with 0.5 µm thickness, the amount of chromium is insufficient (23Cr/6C) and rapidly consumed in the early reaction stages. However, in the case of the thick film (2.64 µm), the amount of chromium is sufficient for the stability of this carbide which is explained by the appearance of many diffraction peaks.

The formation of $Cr_{23}C_6$ and Cr_7C_3 mixture was also observed in the niobium–chromium carbide coatings deposited using the thermo-reactive diffusion deposition technique on AISI D2 steel substrates by Castillejo *et al.*[8] The $Cr_{23}C_6$, also, was detected in the chromium films obtained by diffusion of metallic chromium and iron (III) in another study.[14] However, the Cr_3C_2 compound was not observed.

Hence it is confirmed by the X-Ray microanalysis that the diffusion of carbon from the substrate is solely responsible for formation of these carbides in the deposited coatings. Since the carbon necessary for chromium carbides formation is supplied by the substrate, it is important to determine if the diffusion of carbon from the substrate towards the film leads to a significant carbon concentration gradient near the interface zone between the Cr film and the XC 100 substrate.

EDS analysis was used to determine the concentration profile for iron, chromium, carbon and oxygen in the samples at different annealing temperatures (Figure 2). It is observed from Figure 2, that the carbon concentration increases due to its diffusion towards the surface. This leads to a higher mobility of smaller carbon atoms which explains the rapid reaction and formation of different chromium carbides during the annealing treatment.

Figure 2 also shows the decrease of chromium concentration and the increase in the iron concentration near the interface from 900°C due to their reversible diffusion between the coating and the substrate caused by the transformation of binary carbide Cr_7C_3 to the ternary carbide $(Cr, Fe)_7C_3$ at higher temperatures. The annealing treatment of 950°C favours the formation of chromium carbides and improves the element inter-diffusion across the substrate/coating interface.[16]

This may be explained by two main factors, namely the influence of atomic size and the diffusion activation energy. It is known that the size effect plays an important role in the diffusion phenomenon. The carbon atom has an atomic radius ($Ra_C = 0.7$ Å) smaller than that of chromium, ($Ra_{Cr} = 1.4$ Å), iron ($Ra_{Fe} = 1.4$) and oxygen ($Ra_O = 0.7$) atoms, respectively, because of which it diffuses easily in chromium and iron. But, if we consider the activation energy, it is identified that the diffusion flow of carbon is higher in chromium than that in iron. This is clarified by the fact that the diffusion activation energy of carbon into polycrystalline chromium is 1.15 eV and that in polycrystalline iron is 1.41 eV,[17] leading to the conclusion that the diffusion of carbon into chromium needs lower energy than its diffusion in iron.

So, for the same annealing temperature, the diffusion of carbon is more effective in chromium than in iron. On the other hand, the diffusion activation energy of chromium into polycrystalline iron (3.45 eV)[16] is three times higher than the diffusion energy of carbon into polycrystalline chromium (1.15 eV)[16] which justifies the fact that the increase of diffusion flow of carbon from the substrate towards the coating has preceded the diffusion of chromium from the coating towards the substrate. The formation of chromium carbides happens in the (coating/substrate) interface and sometimes it also forms in the chromium coating. But the rapid transformation from these binary carbides to the ternary carbides caused by the high energy obtained from annealing treatment and the existence of crystallographic point defects has an effect on the appearance of grain boundaries. Nevertheless, the critical oxygen concentration at higher annealing temperatures (800 and 900°C), reducing from 12 to 8 at.-%, was mainly located in the film, and which partly

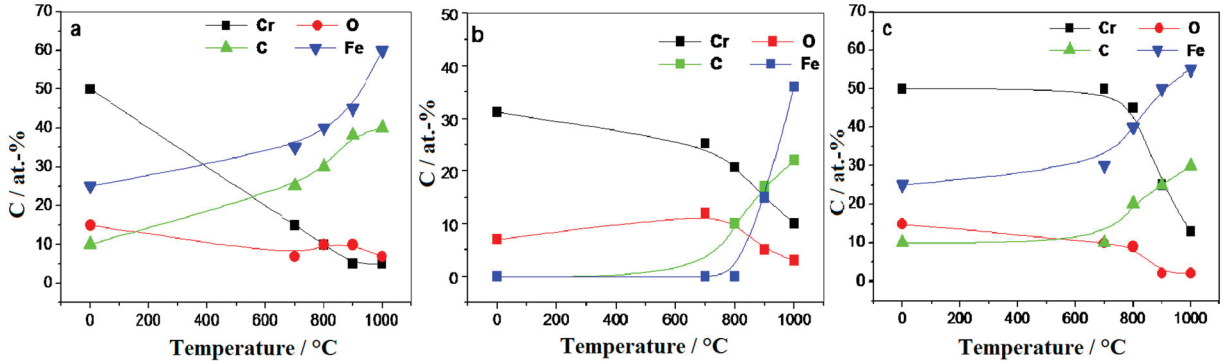

Figure 2. EDS profile analysis of Cr, Fe, C and O elements for: (a) 0.5 µm Cr/XC100, (b) 1.13 µm Cr/XC100 and (c) 2.64 µm Cr/XC100 after annealing.

replaces the carbon. This oxygen contamination probably originates from oxides stability until the temperature reaches 800°C.

Figure 3 displays the XPS spectra of Cr2p, and C1s of Cr/XC100 film at 900°C for each one of the films with different thicknesses. It is observed that the $Cr2p_{3/2}$ peak is located at 574.6 eV of energy in the case of the 0.5 µm Cr/XC100 sample and at a binding energy of about 575.1 eV in the case of 1.13 µm Cr/XC100 and 2.64 µm Cr/XC100 samples. According to M. Fellah *et al.*[18] the Cr peaks located exactly at 574.4 eV correspond to metal Cr–Cr bonds. In this study, the Cr2p peak is shifted to higher binding energies. These binding energies represent the mixture of Cr_7C_3 and $Cr_{23}C_6$ chromium carbides, due to the transformation of chromium into chromium carbide which is related to the transfer charge phenomena of Cr–Cr to Cr–C atoms. It can also be seen that the C1s peak shape is not symmetric. This is due to the contribution of several carbon bonds: the C–C bond of free carbon with the Cr–C bond of chromium carbides which is dominant at 283.5 eV.[19]

The formation of microstructure during the annealing treatment of chromium films was examined using SEM. The results are as shown in Figure 4. It can be clearly observed that before heat treatment, the surface cracks gradually disappeared with increasing film thickness and the surface becomes compact and homogeneous with a columnar structure at a film thickness of 2.64 µm (Figure 4(c)). During heat treatment, the increasing of the film thickness encourages the grain coalescence in coatings due to the high mobility and rapid diffusion of atoms.

After annealing at 1000°C, the surface topography presents rough film surfaces (Ra ≈ 103 nm). The SEM observations reveal a dense morphology, consisting of globular grains. However, no occurrence of cracks or micropores was observed on the 2.64 µm thick film, showing the excellent thermal stability of this film at higher temperatures. However, micropores appear on the film surface of 1.13 µm Cr/XC100 sample (Figure 4(b)), which can be attributed to the significant diffusion of Cr atoms towards the XC100 steel substrate.

Moreover, it is also observed that an increase in the annealing temperature results in a particular morphology of the thin films (0.5 µm Cr/XC 100) (Figure 4(a)). This may be due to the grain coalescence accompanied by a cracking of their uniform morphology layer. This behaviour appears as dark areas in Figure 4(a), which makes up the rest of the grains. These zones are surrounded by clear bands centred on the grain boundary; containing an important cracks charge. This may have been caused by the existence of internal stresses. Therefore, the increasing of defects density in the Cr thin films can be attributed to the greater diffusion of Cr atoms from the film, which leads to the decrease of its density leading to a relaxation of internal stresses. This structure was also observed by Gheriani *et al.* in chromium coatings deposited by magnetron sputtering technique.[20]

The variation of the d-spacing parameters (d_{hkl}) of the Cr_7C_3 (202) diffraction peak, was calculated using the Bragg formula, as a function of film thickness after annealing between 900 and1000°C (Figure 5).

A decrease in d-spacing parameters is observed with increasing film thickness and annealing temperature, giving a value close to that of Cr_7C_3 (202) solid carbide (7.38 Å) for 2.64 µm thick film after annealing at 1000°C (Figure 5(a)), indicating a microstructural improvement and a stoichiometry of the Cr–C film with raising the annealing temperature. Also, the increasing of the crystallite size with increasing film thickness can be explained by the rapid consumption of Cr thin films due to its low density and high defects concentration (Figure 5(b)).

With increasing of annealing temperature from 900 to 1000°C, the crystallite size and the film thickness were found to be increased. So, the decrease of the inter-reticular distance (d_{hkl}) and the increase of grain size with increasing the annealing temperature in the Cr–C film could be possibly due to the fact that the high thermal annealing provides the necessary energy to the Cr and C atoms for rearranging in crystal lattices and in space lattice sites.

3.2. Mechanical properties

Film thickness is one of the parameters that can influence the stress levels. In the present case, the authors wanted to verify that the order of micron film thicknesses presented a low residual stress (Figure 6). For this, a Cr film was deposited with a uniform deposition speed. It is observed that the tensile residual stress in the Cr films is low which is explained by the large presence of oxygen in the external surface. The residual stresses take a maximum value at a film thickness of 180 nm and relax progressively, stabilising at 0.5 GPa from 1 µm thickness and above. The residual stress of base chromium films on steel was calculated by Eigenmann *et al.*[1] using X-ray spectra.

According to Nouveau *et al.*[21] who observed the same result on CrN film deposited by magnetron sputtering

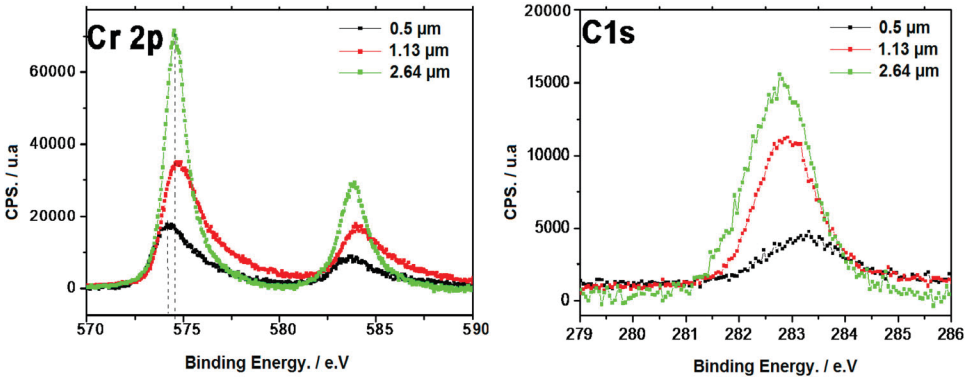

Figure 3. XPS spectra of Cr/XC100 sample for different thicknesses; after annealing at 900°C.

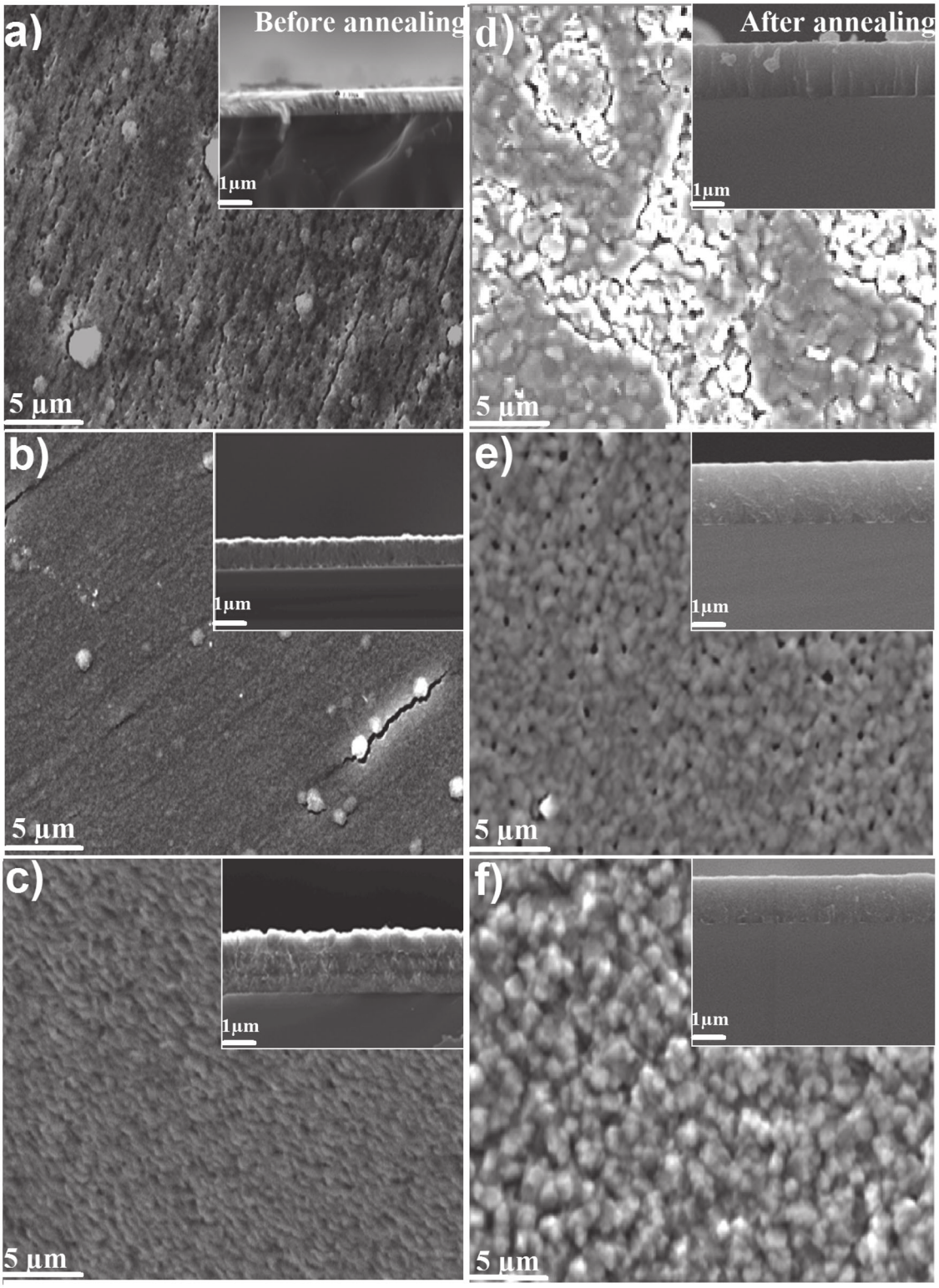

Figure 4. SEM micrographs of the surfaces and cross-section before annealing of: (a) 0.5 µm Cr/XC100, (b) 1.13 µm Cr/XC100, (c) 2.64 µm Cr/XC 100 and after annealing at 1000°C for 1 h of: (d) 0.5 µm Cr/XC100, (e) 1.13 µm Cr/XC100 and (f) 2.64 µm Cr/XC100.

technique, the decrease of the stress with increasing thickness is explained by the shadowing effect. The latter is responsible for the creation of inter-columnar voids that relax the stress level. In fact, Hones[22] explained this process by the transition growth from cylindrical columns to conical columns, inducing shadow effects during deposition and hence voids increasingly become important when the thickness of the layer increases.

The optimisation of the mechanical properties like hardness and Young's Modulus of metallic thin films is very important, given their important industrial applications. Figure 7 illustrates the results of the nano-indentation measurements. The general shapes of the indentation curve for Cr/XC100 samples are the same. The evolution of the hardness curve starts with a slight increase which is probably due to the formation of chromium oxide (Cr_2O_3) which stabilises mainly at 800°C, followed by a sudden increase at between 800 and 900°C, reaching a maximum value of about 25 GPa in the case of 2.64 µm thick films. The rapid increase in hardness (for all three thicknesses) in this interval can be attributed

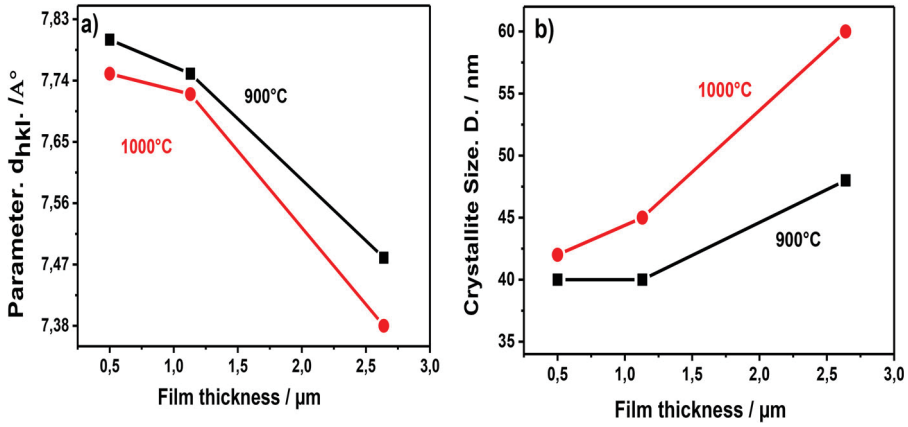

Figure 5. Evolution of: (a) d parameter and (b) the crystallite size of the Cr film with film thickness after annealing temperature at 900 and 1000°C for 1 h.

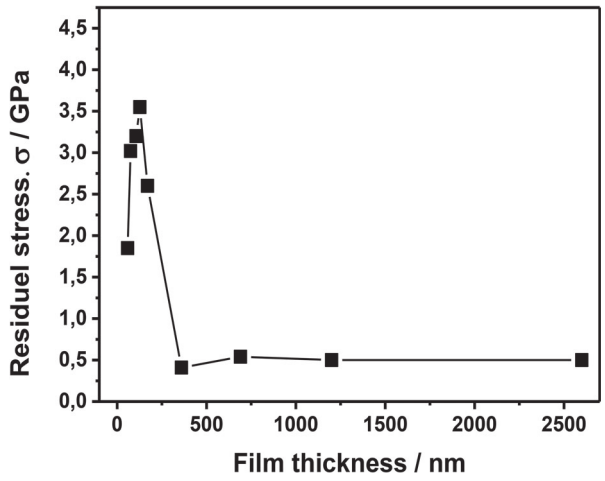

Figure 6. Residual stress of Cr films before annealing.

to the formation of the hardest carbide (Cr_7C_3). A significant difference between the mechanical properties values with the increase of the film thickness is also observed. Hardness and Young's Modulus values of ($H = 12$ GPa, $E = 250$ GPa), ($H = 18$ GPa, $E = 320$ GPa) and ($H = 25$ GPa, $E = 330$ GPa) for 0.5, 1.13 and 2.64 µm thickness, respectively, are observed. This can be explained by the low density (in the case of thin film) due to the significant diffusion through grain boundaries (Figure 2), and the high elemental reaction in the case of the film of 2.64 µm thickness. The improvement in hardness by heat treatment was also observed by Poletika *et al.*[11] in the electron beam deposition of tungsten carbide.

Finally, a slight decrease in the mechanical properties between 900 and 1000°C was observed, because of the decrease in the chromium carbides (Cr_7C_3) concentration which is formed on the surface, and its transformation to ternary chromium carbide, especially in the thin film, since it is bound by the iron atoms which diffuse through the surface of the substrate because of the proximity of the atomic lattices of iron and chromium and the formation of binary $Cr_{23}C_6$ carbides which are less hard than the Cr_7C_3 carbide.

The thickness effect is significant, given the fact that a load of 10 g was used which is quite small. The variation of the hardness as a function of the depth of penetration of Cr films at 900°C (Figure 8) shows that the hardness increases up to a maximum value ($H = 12$, 18 and 25 GPa), then it remains constant at the thickness range of 250, 400 and 750 nm for 0.5, 1.13 and 2.64 µm of film thickness, respectively, Then it decreases gradually to 10 GPa (hardness value of XC100 substrate), due to the formation of binary chromium carbides by the diffusion of C, thus increasing the resistance to penetration in this film region. However, the most important cause for the decrease in mechanical properties is the reduction of carbon concentration in the substrate following its diffusion into the film and the formation of carbides. This causes the formation of a fragile interfacial zone between the coating and the substrate which consists of a poor ferritic matrix of carbon.

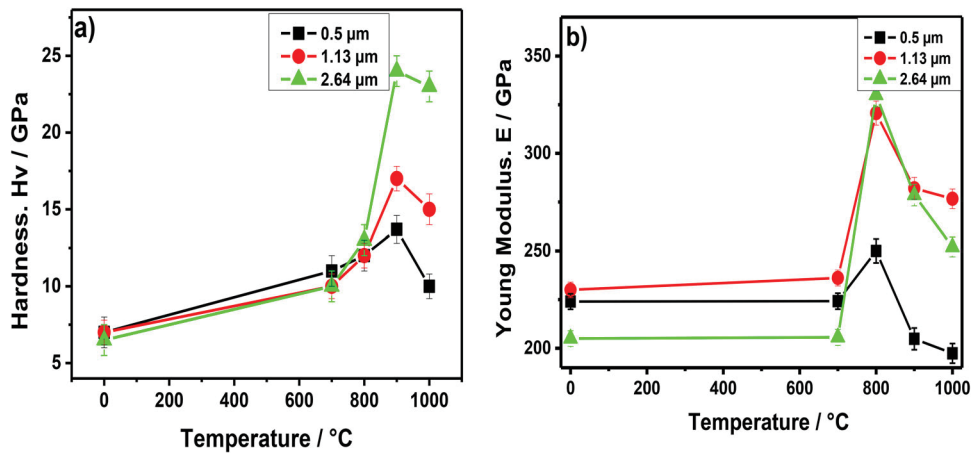

Figure 7. (a) Hardness and (b) Young's Modulus of the Cr films.

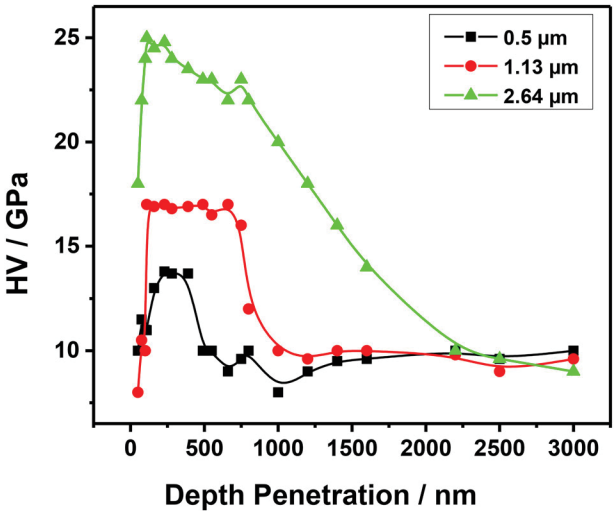

Figure 8. Hardness evolution as a function of the depth penetration of the Cr films.

4. Conclusions

The thermal treatment effect on structural and mechanical properties of Cr–C coatings deposited by magnetron sputtering on high carbon steel substrates has been studied, and the following conclusions can be drawn:

(i) The binary Cr_7C_3 carbide is formed at 800°C, which is transformed to ternary carbide at 1000°C, due to the substitution of iron.
(ii) The $Cr_{23}C_6$ carbide appears only at temperatures greater than 900°C.
(iii) With an increase in the annealing temperature from 900 to 1000°C, the crystallite size was found to increase along with an increase in the film thickness.
(iv) A decrease in d_{hkl}-spacing is observed with increasing film thickness and annealing temperature which takes a value of 7.38 Å at 1000°C
(v) The rapid increase in hardness for samples annealed at 1000°C can be attributed to the formation of the hardest carbide (Cr_7C_3).
(vi) Increases in the hardness and the Young's Modulus values to reach highest values of ($H = 25$ GPa and $E = 330$ GPa), can be attributed to the high elemental reaction in the case of films with 2.64 µm thickness.
(vii) The Young's Modulus measurement is in good correlation with the hardness results, and it can be concluded that it strongly depends on the elasticity state and on the structure of the chromium films.

ORCID

M. Fellah http://orcid.org/0000-0003-0615-6711

References

1. B. Eigenmann, B. Scholtes and E. Macherauch: *Surf. Eng.*, 1991, 7, (3), 221–224.
2. M. Fellah, M. Abdul Samad, M. Labaïz, O. Assala and A. Iost: *Tribol. Internat.*, 2015, 91, 151–159.
3. G. M. Wilson, S. O. Saied and S. K. Field: *Thin Solid Films*, 2007, 515, 7820–7828.
4. F. Maury: *Electrochim. Acta*, 2005, 50, 4525–4530.
5. F. I. Danilov, V. S. Protsenko, V. O. Gordiienko, S. C. Kwon, J. Y. Lee and M. Kim: *Appl. Surf. Sci.*, 2011, 257, 8048–8053.
6. M. Fellah, M. Labaïz, O. Assala, L. Dekhil and A. Iost: *Tribol.-Mater., Surf. Interfaces*, 2013, 7, (3), 135–149.
7. Y. F. Zhou, Y. L. Yang, J. Yang, P. F. Zhang, X. W. Qi, X. J. Ren and Q. X. Yang: *Surf. Eng.*, 2013, 29, (5), 366–373.
8. F. E. Castillejo, D. M. Marulanda, J. J. Olaya and J. E. Alfonso: *Surf. Coat. Technol.*, 2014, 254, 104–111.
9. L. Aissani, C. Nouveau, M. J. Walock, H. Djebaili and A. Djelloul: *Surf. Eng.*, 2015, 31, (10), 779–788.
10. M. R. R. Junqueira, C. R.O. Loureiro, M. S. Andrade and V. T.L. Buono: *Surf. Coat. Technol.*, 2009, 203, 1908–1912.
11. I. M. Poletika, T. A. Krylova, M. V. Tetyutskaya and S. A. Makarov: *Welding Internat.*, 2013, 27, (7), 508–515.
12. M. Fellah, M. Labaïz and O. Assala: 'Tribological Behavior of Friction Couple: Metal/Ceramic (Used for Head of Total Hip Replacement)'. John Wiley & Sons, Inc., USA. Advances in Bioceramics and Porous Ceramics VI, Vol. 34 (6) (2013) 45–57.
13. Z. Wang, H. Wang, S. Wang and J. Liu: *Sci. Technol. Adv. Mater.*, 2001, 2, (1), 297–302.
14. M. Kolnes, J. Pirso, J. Kübarsepp, M. Viljus and R. Traksmaa: *Mater. Eng.*, 2016, 65, (2), 138–143.
15. L. Aissani, M. Fellah, M. Abdul Samed, N. Corinne and A. Montagne: *Surf. Eng.*, 2017, 33, (09), DOI:10.1080/02670844.2017.1338378
16. Y.-X. Xu, X.-T. Luo, C.-X. Li, G.-J. Yang and C.-J. Li: *Surf. Eng.*, DOI:10.1080/02670844.2016.1202672.2016.
17. W. V. Geertruyden and D. W. Hetzner: *Mater. Characteris.*, 2008, 59, 825–841.
18. M. Fellah, L. Aissani, N. Corinne, M. Abdul Samed and A. Montagne: *Trans. IMF*, 2017, 95, (05), 261–268. DOI:10.1080/00794236.2017.1339464.
19. T. Jiang, I. Odnevall and G. Herting: 'Chemical Stability of Chromium Carbide and Chromium Nitride Powders Compared with Chromium Metal in Synthetic Biological Solutions'. ISRN Corrosion 2012, (2012), ID 379697.
20. R. Gheriani, R. Halimi and R. Bensaha: *Surf. Coat. Technol.*, 2004, 180–181, 49–52.
21. C. Nouveau, M. A. Djouadi and C. Décès-Petit: *Surf. Coat. Technol.*, 2003, 174–175, 455–460.
22. M. Fellah, L. Aissani, M. Abdul Samad, A. Purnama, H. Djbaili, A. Montagne, A. Iost and C. Nouveau: *Int. J. Appl. Ceram. Tec.*, 2017, DOI:10.1111/ijac.12833.